Accelerated Publications

Structure of KCNE1 and Implications for How It Modulates the KCNQ1 Potassium Channel[†,‡]

Congbao Kang,[§,||] Changlin Tian,[§,||,⊥] Frank D. Sönnichsen,[@,#] Jarrod A. Smith,[§] Jens Meiler,[∇,●] Alfred L. George, Jr.,[∇,+] Carlos G. Vanoye,[∇,+] Hak Jun Kim,[§,○] and Charles R. Sanders*[,§]

Departments of Biochemistry, Pharmacology, Chemistry, and Medicine, Vanderbilt University, Nashville, Tennessee 37232, Department of Physiology and Biophysics, Case Western Reserve University, Cleveland, Ohio 44106, and Department of Chemistry, Christian Albrechts University, Kiel, Germany

Received May 12, 2008; Revised Manuscript Received June 16, 2008

ABSTRACT: KCNE1 is a single-span membrane protein that modulates the voltage-gated potassium channel KCNQ1 (K_V7.1) by slowing activation and enhancing channel conductance to generate the slow delayed rectifier current (I_{Ks}) that is critical for the repolarization phase of the cardiac action potential. Perturbation of channel function by inherited mutations in KCNE1 or KCNQ1 results in increased susceptibility to cardiac arrhythmias and sudden death with or without accompanying deafness. Here, we present the three-dimensional structure of KCNE1. The transmembrane domain (TMD) of KCNE1 is a curved α-helix and is flanked by intra- and extracellular domains comprised of α-helices joined by flexible linkers. Experimentally restrained docking of the KCNE1 TMD to a closed state model of KCNQ1 suggests that KCNE1 slows channel activation by sitting on and restricting the movement of the S4−S5 linker that connects the voltage sensor to the pore domain. We postulate that this is an adhesive interaction that must be disrupted before the channel can be opened in response to membrane depolarization. Docking to open KCNQ1 indicates that the extracellular end of the KCNE1 TMD forms an interface with an intersubunit cleft in the channel that is associated with most known gain-of-function disease mutations. Binding of KCNE1 to this "gain-of-function cleft" may explain how it increases conductance and stabilizes the open state. These working models for the KCNE1−KCNQ1 complexes may be used to formulate testable hypotheses for the molecular bases of disease phenotypes associated with the dozens of known inherited mutations in KCNE1 and KCNQ1.

KCNE1 (previously called minK) belongs to the KCNE family of single-span membrane proteins that modulate the activity of several voltage-gated K^+ channels, including KCNQ1 (K_V7.1). In cardiac myocytes, KCNE1 forms obligate complexes with KCNQ1 to generate the slowly activating cardiac delayed rectifier current (I_{Ks}), a critical determinant of myocardial repolarization (*1–3*). In the cochlea, this same channel complex enables secretion of K^+ into endolymph and is critical for hearing (*4*). KCNE1 modulates KCNQ1 function by slowing voltage-stimulated channel activation, increasing conductance, and eliminating channel inactivation (*2*). The relevance of KCNE1 to proper channel function is underscored by heritable mutations in KCNE1 that are linked to congenital long QT syndrome (LQTS)[1] and deafness (*5–9*). Although a number of structures of K^+ channels and cytosolic channel accessory proteins have been determined (*10–12*), as have structures for cytosolic domains of KCNQ family members (*13, 14*), little information exists regarding the structure of KCNE1 or any other transmembrane channel regulatory subunit belonging to the KCNE family. Here, we report the three-dimensional structure of full-length human KCNE1 in model membranes and propose a working structural model for how the transmem-

[†] This work was supported by NIH RO1 Grants DC007416 (C.R.S.) and HL077188 (A.L.G.), by an American Heart Association fellowship (C.T., 0625586B), and by Chinese National Science Research Plan 2006CB910204 (C.T.).

[‡] Coordinates for the structure of KCNE1 have been deposited in the Protein Data Bank as entry 2k21.

* To whom correspondence should be addressed. Telephone: (615) 936-3756. Fax: (615) 936-2211. E-mail: chuck.sanders@vanderbilt.edu.

[§] Department of Biochemistry, Vanderbilt University.

[||] These authors contributed equally to this work.

[⊥] Current address: School of Life Science, University of Science and Technology of China, Hefei, Anhui 230026, China.

[@] Case Western Reserve University.

[#] Christian Albrechts University.

[∇] Department of Pharmacology, Vanderbilt University.

[●] Department of Chemistry, Vanderbilt University.

[+] Department of Medicine, Vanderbilt University.

[○] Current address: Korea Polar Research Institute, Incheon 406-840, Korea.

[1] Abbreviations: GOF, gain-of-function; LMPG, lyso-myristoylphosphatidylglycerol; LQTS, long-QT syndrome; NMR, nuclear magnetic resonance; PRE, paramagnetic relaxation enhancement; RDC, residual dipolar coupling; rmsd, root-mean-square deviation; TMD, transmembrane domain; TROSY, transverse relaxation-optimized spectroscopy.

10.1021/bi800875q CCC: $40.75
Published on Web 07/09/2008

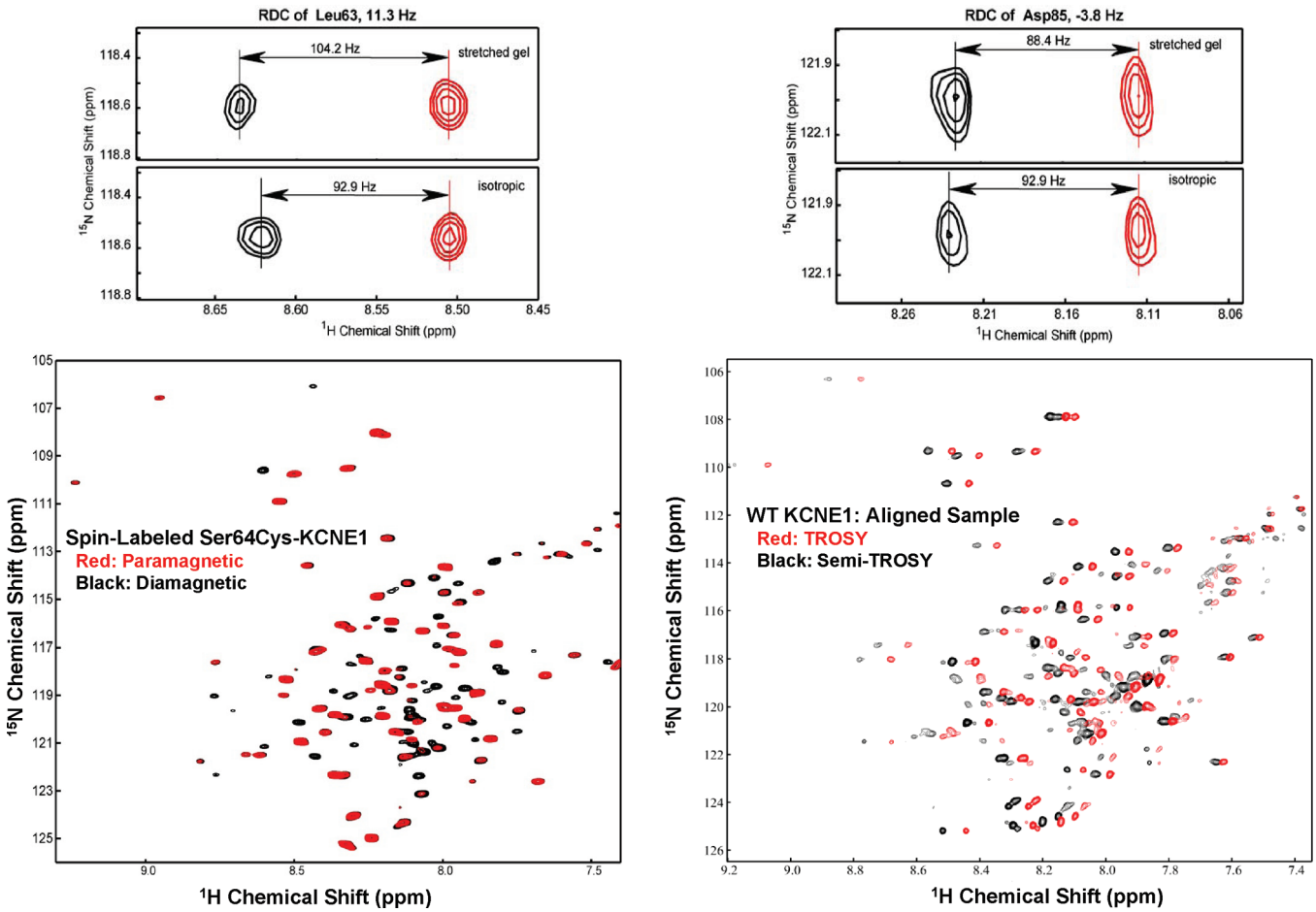

FIGURE 1: Examples of NMR data from which structural restraints were derived for KCNE1. All spectra were acquired for uniformly ^{15}N-labeled KCNE1 in LMPG micelles at 40 °C and pH 6.0. The bottom left panel is an example of data used to obtain paramagnetic relaxation enhancement-derived distances. The 600 MHz TROSY spectra from KCNE1 are shown before (paramagnetic) and after (diamagnetic) reduction of a nitroxide spin-label attached to the side chain of Cys64 in the Cys105Ala/Ser64Cys single-cysteine mutant form of KCNE1. The bottom right panel are superimposed 800 MHz TROSY and semi-TROSY spectra of wild-type KCNE1 that was marginally aligned within a stretched 5% polyacrylamide gel. Not shown is the corresponding pair of spectra from an unaligned sample. Doublets from both pairs of spectra were used as illustrated in the top panel to determine the ^{1}H−^{15}N residual dipolar couplings [for Leu63 (left) and Asp85 (right)] by subtracting the J coupling measured in the isotropic spectra from the $J + D$ coupling observed in the aligned spectra. Additional technical details are presented in the Supporting Information.

brane domain of this accessory protein contributes to modulation of KCNQ1.

MATERIALS AND METHODS

Abbreviated materials and methods are presented in this section. Full details are provided in the Supporting Information.

Determination of the KCNE1 Structure. Human KCNE1 was expressed in *Escherichia coli*, purified into LMPG micelles, and prepared for solution NMR spectroscopy at pH 6.5 and 45 °C as described previously (*15*). Resonance assignments were previously completed (*15*) and deposited in the BioMagResBank as entry 15102. Backbone structural restraints were acquired in the form of backbone and C_β resonance chemical shifts, residual dipolar couplings (RDCs), and short-range nuclear Overhauser effects. Five different Ser-to-Cys single-cysteine forms of KCNE1 were nitroxide spin-labeled and used to measure paramagnetic relaxation enhancements (PREs) that were converted to amide proton−spin-label distances (*16*). The mutant forms of PMP22 used for the PRE measurements (see the Supporting Information) exhibited only minor changes in TROSY NMR peak positions, indicating little structural perturbation due to the mutations and subsequent chemical modification. Examples of the NMR data from which the PRE and RDC data were acquired are shown in Figure 1. The NMR restraints were used to calculate the three-dimensional structure of KCNE1 using XPLOR-NIH (*17*). Two sets of acceptable structures were initially obtained in which the extramembrane segments of the protein were arranged around the TMD in a topologically quasi-mirror fashion. One of these two sets was deemed to be correct because of better agreement with ^{1}H−^{15}N residual dipolar couplings from the extramembrane domains. These particular couplings were not used in the primary structural determination because of the known flexibility of parts of the extramembrane domains (*15*). A table describing the statistics of the determined KCNE1 structure is provided in the Supporting Information. The coordinate file for a representative of the ensemble that best satisfies all the data was deposited in the Protein Data Bank (entry 2k21) and is available in the Supporting Information.

Data-Restrained Docking of KCNE1 to the KCNQ1 Channel. Twenty low-energy models each for both the open and closed states of the KCNQ1 channel were developed as

described previously (*18*) using a combination of homology modeling and ROSETTA calculations, drawing heavily upon the $K_v2.1$ crystal structure (*10, 18*) and the related ROSETTA models of Yarov-Yarovoy et al. (*19*). The 10 lowest-energy NMR structures of the TMD (sites 45−71) were then docked in backbone-only mode into each of the 40 KCNQ1 structures using ROSETTA-DOCK (*20*) in conjunction with application of very loose experimental/topological restraints. (i) KCNE1 sites 55 and 56 were restrained to be located near the center of the bilayer on the basis of their inaccessibility to reagent added from either side of the membrane (*21*). (ii) KCNE1 has an N-terminal-extracellular/C-terminal-intracellular topology, so it is reasonable to restrict its tilt with respect to the bilayer normal to <50°. (iii) On the basis of single- and double-mutation structure−function complementarity, KCNE1 sites 58 and 59 are thought to be in the proximity of sites 340 and 339 in KCNQ1, respectively (*22*). (iv) On the basis of single- and double-Cys insertion mutagenesis followed by functional testing in the presence and absence of Cd(II), sites 51 and 54 of KCNE1 are believed to be proximal to site 331 of KCNQ1, while site 51 is also believed to be proximal to site 328 of KCNQ1 (*23*). Eighty thousand candidate models were generated, which were then filtered using the experimental restraints described above with more stringent cutoffs, followed by clustering of the structures that satisfied the restraints into structural families. This led to approximately 200 families each for the open and closed states. Representatives from each family were then subjected to additional ROSETTA-DOCK calculations, this time in residue side chain-inclusive mode (*24*). The resulting ca. 3000 models were then refiltered using more even more stringent cutoffs for the experimental restraints and also additional open state-specific restraints (see the Supporting Information), which led to the 17 open state models and 28 closed state models (see Results and Discussion). Single representative structures that reflected the mean from each state were selected and subjected to further energy minimization. The PDB coordinates for these models are provided in the Supporting Information.

The key assumptions that were made in developing the models of the KCNE1−KCNQ1 complexes described above are as follows: (i) the KCNQ1 open and closed state models are essentially correct, (ii) the presence of KCNE1 does not perturb the structures of KCNQ1's open and closed states, (iii) the conformation of the KCNE1 TMD observed in LMPG micelles is retained when bound to KCNQ1, and (iv) those experimental restraints that were applied to both the open and closed states are equally applicable to both states.

RESULTS AND DISCUSSION

Structure of KCNE1. Using solution NMR, we determined the backbone structure of human KCNE1 in LMPG micelles, a model membrane system that was previously deemed to be well-suited for studies of KCNE1 from both NMR and protein functional standpoints (*15*). KCNE1 is seen to be comprised of an α-helical transmembrane domain (TMD, residues 45−71) and flanking N- and C-termini that consist of a series of flexibly linked α-helices, with the distal C-terminus (residues 107−129) being disordered (Figure 2). The observed conformation of KCNE1 appears to reflect the micellar environment in which the NMR studies of the protein were carried out, which has previously been observed for some other membrane proteins in micelles (*25–27*). The overall shape of the protein is roughly spherical (Figure 2A), yet the various segments are not compacted as in a well-folded globular protein. Subsequent rigid body docking of the NMR-determined structure into a 36 Å sphere that likely approximates the dimensions of an LMPG micelle leads to a model in which most extramembrane helices are situated on or near the micelle surface (Figure 2C). This model reflects the amphipathicity of the helix spanning residues 12−23 and the presence of a net positive charge for the helix spanning residues 92−106, properties that confer affinity for the negatively charged surface of LMPG micelles. Flexible linkage of the extramembrane helices may allow structural adaptation to KCNE1's local environment that, under physiological conditions, will be defined primarily by how it interacts with KCNQ1.

The observed disorder of the distal C-terminus (Figure 2) is consistent with previous NMR relaxation data (*15*) and with the observation that this intracellular segment can be removed without perturbing normal KCNE1 modulation of KCNQ1 function (*28*). However, disordered segments are often involved in protein−protein recognition (*29*), and the distal C-terminus of KCNE1 is known to undergo interactions with nonchannel proteins in cells (*30*), which may explain the presence of disease-linked mutation sites (Val109 and Pro127) in this domain (*15*).

The KCNE1 juxtamembrane C-terminal domain contributes to the modulation of KCNQ1 and is also important for preventing channel inactivation (*9, 28*), whereas the N-terminus of KCNE1 alters the pH sensitivity and pharmacological profile of the channel (*31, 32*). As illustrated in Figure 3A, it is possible that the flexibly linked helices from either or both termini may form an interface that spans multiple subunits of the channel to preclude binding of more than two KCNE1 subunits to any single tetrameric channel. This suggests an explanation for the known 2:4 stoichiometry of the fully assembled KCNE1−KCNQ1 channel complex (*33, 34*). Elucidating the details of the interactions of the KCNE1 N- and C-terminal helices with KCNQ1 will require future investigations.

The KCNE1 TMD was the most precisely determined domain of the structure (Figure 2D) and has the greatest immediate interest because a number of determinants for modulation of channel activation reside in this segment (*35–37*). That the TMD of full-length KCNE1 in LMPG micelles is helical agrees with the conclusion from previous biophysical studies of the isolated TMD polypeptide (*38–40*). However, what is novel and important about the structure introduced here is that the KCNE1 TMD is seen to adopt a curved helical conformation (Figure 2D), the detection of which reflects the power of residual dipolar coupling and paramagnetic relaxation enhancement NMR measurements. While the possibility that this curvature could arise from micelle-specific distortion cannot yet be ruled out, this seems unlikely because the diameter of LMPG micelles is expected to be similar to the span of native membranes as a result of the long (C14) saturated acyl chain of LMPG. Instead, the curvature likely arises from the backbone conformational balance between glycines located in the TMD and a number of β-branched amino acids also located therein (Figure 3B). It is noteworthy that the side chain of Thr58, a

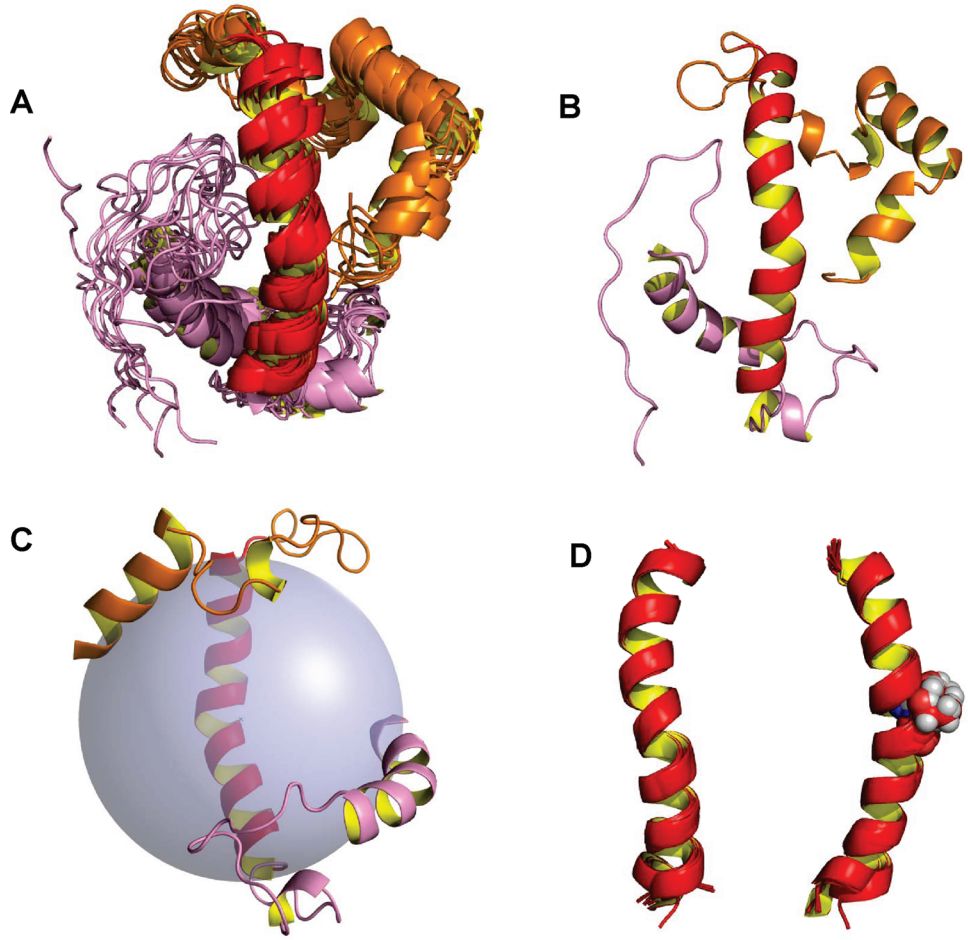

FIGURE 2: Structure of KCNE1. See the Supporting Information for experimental details of structural determination. (A) Ensemble of the 10 lowest-energy conformations determined by NMR (front view). Conformers were overlaid on the basis of minimization of the rmsd over the entire molecule, excluding the disordered C-terminus. The N-terminus is colored orange, the transmembrane domain red, and the C-terminus pink. (B) Representative single structure from the lowest-energy ensemble (front view). (C) Results of rigid body docking of the NMR-determined KCNE1 structure (back view, residues 11−107 only) into a 36 Å sphere that represents the expected dimensions of an LMPG micelle. The actual size and shape of LMPG micelles remain to be experimentally determined. (D) Front and side views of the overlaid transmembrane domains of the 10 lowest-energy structures. In this case, the depicted overlay is based on minimization of the rmsd of the transmembrane domain only. The side chain for Thr58 is depicted in van der Waals mode.

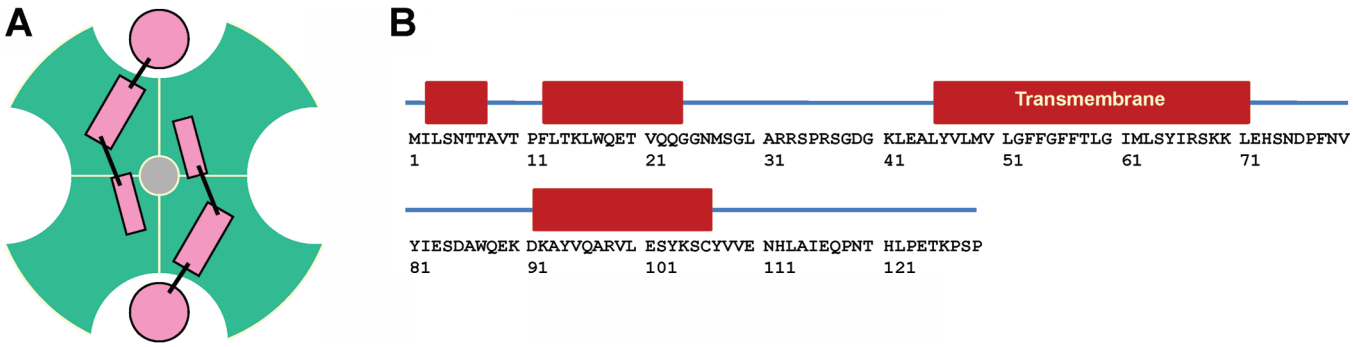

FIGURE 3: (A) Structurally based schematic that may explain the known 2:4 stoichiometry of the fully assembled KCNE1−KCNQ1 complex (extramembrane view). The KCNQ1 tetramer is illustrated by the green shapes. The α-helical KCNE1 TMD is illustrated as a pink circle, and the connecting lines and pink rectangles indicate hypothetical locations of the N- and/or C-termini from two KCNE1 subunits. (B) Sequence of KCNE1, with the NMR-determined locations of α-helices represented as red boxes.

residue that is central in the distinct modulatory effects of KCNE1 relative to its homologue KCNE3 (*22, 36*), is located at the apex of the outer face of the curved helix and is well-exposed to interact with KCNQ1 (Figure 2D). It should be noted that the results of the structural calculations did not support our earlier suggestion that the transmembrane helix of KCNE1 undergoes a break in helicity around sites 59−61 (*15*). The previous conclusion was based largely on NMR relaxation data that indicate an increase in the local backbone dynamics for those sites. This apparent discord in data interpretation may be reconciled either on the basis of there being increased local mobility at sites 59−61 within an unbroken helix or, more likely, by the presence of conformational exchange between a curved unbroken helix and a less-populated structure in which there is a break at sites 59−61.

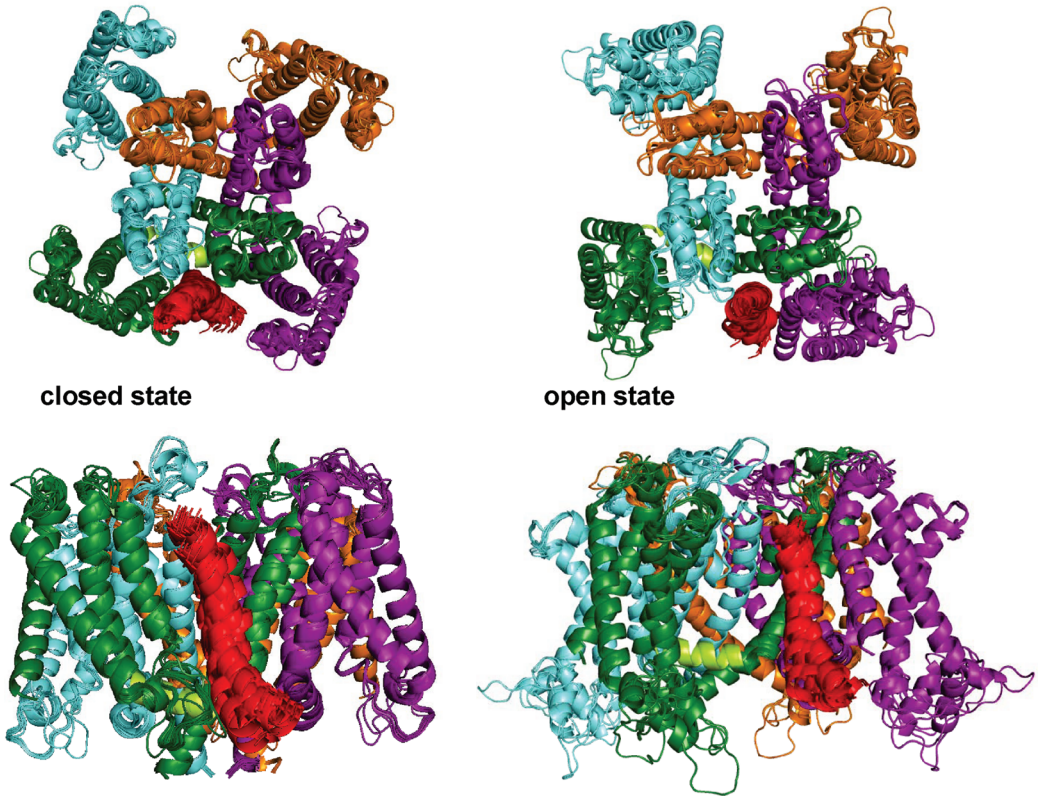

FIGURE 4: Ribbon diagram depictions of the 17 open state models and 28 closed state models of the KCNE1−KCNQ1 complex that were generated by high-resolution (side chain-inclusive) docking and found to be consistent with a series of experimental restraints. The transmembrane domain of KCNE1 (residues 45−71) is colored red, while the four KCNQ1 subunits are colored blue, orange, purple, and green.

Mechanisms of KCNE1 Modulation of KCNQ1 Channel Function. To potentially gain insight into how KCNE1 slows channel activation and enhances conductance, we used ROSETTA (*20, 24*) to perform ensemble docking of the 10 lowest-energy experimental KCNE1 TMD structures into each member of a previously developed ensemble of 20 low-energy KCNQ1 models (*18*) for both open and closed channel states. These channel models were developed in a manner that relied heavily on the approach taken by Yarov-Yarovoy et al. in their studies of the homologous $K_v1.2$ potassium channel (*19*). As described in detail in the Supporting Information, this first phase of docking resulted in 80000 models for the complex that were then filtered to select models that satisfy experimentally derived restraints for the vertical placement of KCNE1 with respect to the center of the membrane (*21*) and for $C_\beta-C_\beta$ distances between specific KCNE1−KCNQ1 residue pairs (*22, 23*). In addition, we also employed open state-specific interresidue distance restraints from recent disulfide mapping studies (*41, 42*). These experimentally derived restraint filters resulted in the selection of precisely converged structure ensembles for the closed and open states as depicted in Figure 4. Figure 5 shows a representative pair of complexes that resemble the average for the open and closed state KCNE1−KCNQ1 ensembles. For both models, we observed that KCNE1 forms direct contacts with the S5−P−S6 pore domain and sits in a cleft between this pore domain and an adjacent voltage sensor. These findings are consistent with prior work that demonstrated the S5−P−S6 domain to be critical for the biochemical interaction between KCNQ1 and KCNE1 (*22, 36, 43*). However, the cleft occupied by KCNE1 in the closed state is different from the one occupied in the open state. Videos were prepared that show the structural trajectory for the transition from the closed to open channel state, based on simple linear extrapolation of atomic positions (videos 1 and 2 of the Supporting Information). While these videos do not represent an attempt to elucidate the transition state for the interconversion between open and closed conformations, the fact that the geometrically simplest path for conversion between states does not require any stereochemical abominations, such as atoms or chains passing through each other, is reassuring.

The KCNE1−KCNQ1 models are best regarded as being medium-resolution in nature, both because of the imperfect precision of structures that satisfy the experimental restraints used in docking (see Figure 4) and because of uncertainty regarding some of the assumptions made in the restrained docking calculations (see the end of Materials and Methods). Therefore, a description of these models in terms of specific residue−residue contacts does not appear to be merited. However, even at moderate resolution, the general locations of the KCNE1 TMD with respect to KCNQ1 suggests a compelling mechanism for key aspects of KCNE1 function. In the closed state model (Figure 5), the intracellular end of the KCNE1 TMD sits on the S5 end of the critical S4−S5 linker of KCNQ1 that connects the voltage sensor to the pore domain and is thought to press downward on the cytosolic end of the S6 helix to hold the channel gate in a closed position (*19, 44*). At the same time, the curved nature of KCNE1 enables the upper end of the TMD to form extensive contacts with a cleft formed between the upper part of S3 on the voltage sensor of one KCNQ1 subunit and the S5

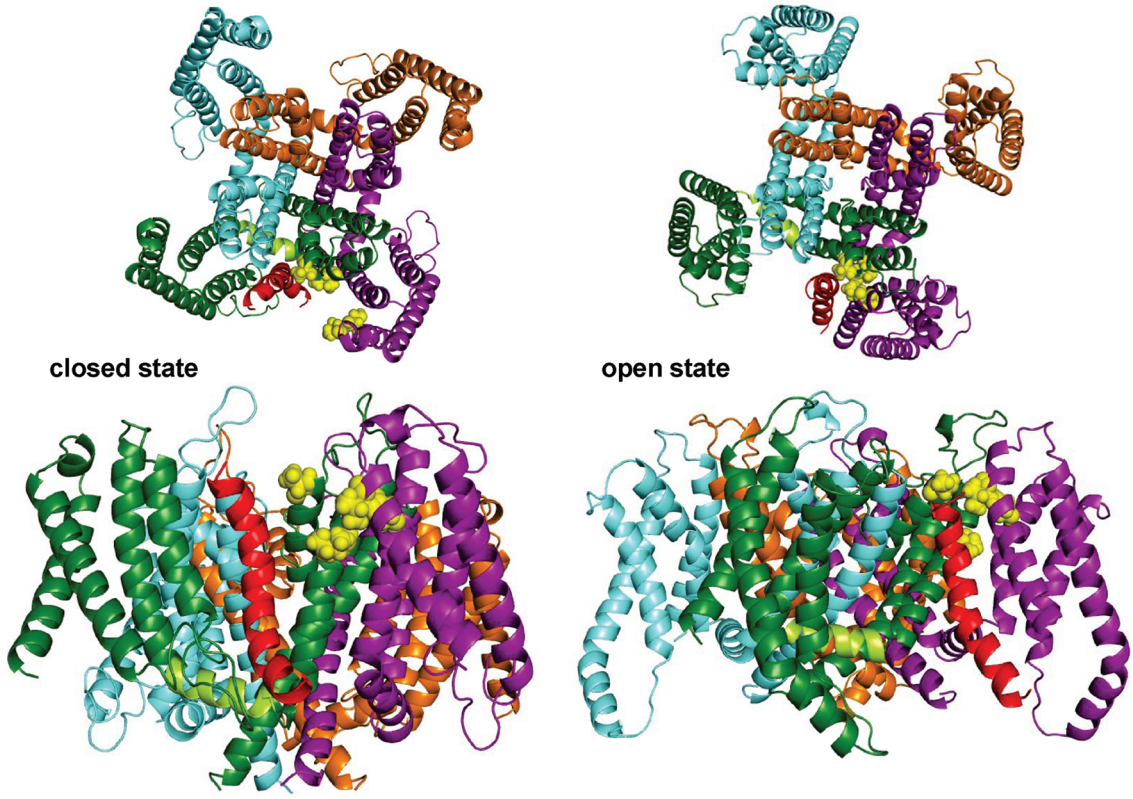

FIGURE 5: Details of the open and closed state KCNE1−KCNQ1 complexes. Ribbon diagrams of representative models for the closed and open state KCNE1−KCNQ1 complexes, as generated by experimentally restrained docking calculations. The transmembrane domain of KCNE1 is colored red. The S4−S5 linker is depicted as a light green helix in the green subunit. The side chains of the four gain-of-channel-function disease mutation sites in a selected GOF cleft are depicted in van der Waals mode (Ser140, Val141, Ile274, and Ala300).

and S6 segments of another. We propose that this extensive contact surface between KCNE1 and KCNQ1 creates an adhesive interface between the two proteins that must be disrupted following membrane depolarization before the S4−S5 linker can be drawn back to allow the S6 gate to spring open. This offers a plausible explanation for how KCNE1 delays KCNQ1 channel activation.

When the KCNQ1−KCNE1 complex makes the transition to the open state, the closed state contacts between the KCNE1 TMD and KCNQ1 are completely disrupted as KCNQ1 rearranges itself around KCNE1, which itself undergoes only modest changes in position, tilt, and rotation (see Supporting Figure 2 and videos 1 and 2). In the open state, the N-terminus of the KCNE1 TMD sits in a cleft that is vertically situated along the bilayer normal at roughly the same level as the selectivity filter and is in contact with three different KCNQ1subunits: S1 from one subunit, S5 and the end of the pore helix from a second subunit, and S6 from a third subunit. Notably, this cleft is the location for four of five known KCNQ1 gain-of-function (GOF) disease-associated mutations (Ser140Gly, Val141Met, Ile274Val, and Ala300Thr) (*6, 45–47*). Moreover, for at least three of four of these mutations, the GOF channel phenotype is observed only when KCNE1 is present (see the Discussion in ref *15*), a condition that is explained by our open channel complex model. In this model, the central domain/C-terminus of the KCNE1 TMD sits at an interface between the cytosolic end of S1 in one subunit and S5 in another. Placement of the N-terminal end of the KCNE1 TMD in this "GOF cleft" likely stabilizes the open state of the channel and enhances conductance. It is also noteworthy that residues near the middle of KCNE1's TMD are in contact with the end of the "elbow" formed by the terminus of S4 and the ensuing S4−S5 linking helix, an interaction that may also stabilize the open channel state and possibly explains KCNE1-induced changes in the state-dependent accessibility of the S4 segment to chemical modifiers (*48, 49*).

In summary, determination of the KCNE1 structure using solution NMR and subsequent experimentally restrained docking of the TMD into the KCNQ1 potassium channel offers a working model for how the TMD of KCNE1 plays a central role in modulating KCNQ1 function. These models and their underlying assumptions will, of course, have to tested by future experimental work. Moreover, the working models also do not directly address the nature of the transition state between the open and closed forms of the channel, which may be the point at which certain residues in KCNE1 and KCNQ1 play their key roles in channel modulation (cf. ref *36*). Our models also do not address how the juxtamembrane C-terminal domain of KCNE1 works in concert with the TMD to modulate KCNQ1 function (*28, 50*), a matter that will also require additional studies. However, as the first semicomprehensive attempt to describe the structural basis for KCNE1's modulation of KCNQ1, it is hoped that the proposed working models for KCNE1−KCNQ1 interactions will provide a lucid basis for generating testable hypotheses regarding both the mechanisms of KCNQ1 channel regulation and the nature of the molecular defects that lead to long-QT syndrome and the other disorders known to result from dysfunction of KCNE1 and KCNQ1.

SUPPORTING INFORMATION AVAILABLE

Full methodological details, a structural quality table, a schematic that outlines the restrained docking protocol used in this work, a figure of the superimposed closed and open state KCNE1−KCNQ1 complexes, supporting videos that show extracellular and membrane views of the interconversion between open and closed state KCNE1−KCNQ1 models, and Protein Data Bank files for the open and closed state KCNE1−KCNQ1 models. This material is available free of charge via the Internet at http://pubs.acs.org.

REFERENCES

1. Barhanin, J., Lesage, F., Guillemare, E., Fink, M., Lazdunski, M., and Romey, G. (1996) K(V)LQT1 and lsK (minK) proteins associate to form the I(Ks) cardiac potassium current. *Nature 384*, 78–80.
2. McCrossan, Z. A., and Abbott, G. W. (2004) The MinK-related peptides. *Neuropharmacology 47*, 787–821.
3. Sanguinetti, M. C., Curran, M. E., Zou, A., Shen, J., Spector, P. S., Atkinson, D. L., and Keating, M. T. (1996) Coassembly of K(V)LQT1 and minK (IsK) proteins to form cardiac I(Ks) potassium channel. *Nature 384*, 80–83.
4. Romey, G., Attali, B., Chouabe, C., Abitbol, I., Guillemare, E., Barhanin, J., and Lazdunski, M. (1997) Molecular mechanism and functional significance of the MinK control of the KvLQT1 channel activity. *J. Biol. Chem. 272*, 16713–16716.
5. Abbott, G. W., and Goldstein, S. A. (2002) Disease-associated mutations in KCNE potassium channel subunits (MiRPs) reveal promiscuous disruption of multiple currents and conservation of mechanism. *FASEB J. 16*, 390–400.
6. Chen, Y. H., Xu, S. J., Bendahhou, S., Wang, X. L., Wang, Y., Xu, W. Y., Jin, H. W., Sun, H., Su, X. Y., Zhuang, Q. N., Yang, Y. Q., Li, Y. B., Liu, Y., Xu, H. J., Li, X. F., Ma, N., Mou, C. P., Chen, Z., Barhanin, J., and Huang, W. (2003) KCNQ1 gain-of-function mutation in familial atrial fibrillation. *Science 299*, 251–254.
7. Jespersen, T., Grunnet, M., and Olesen, S. P. (2005) The KCNQ1 potassium channel: From gene to physiological function. *Physiology 20*, 408–416.
8. Peters, T. A., Monnens, L. A., Cremers, C. W., and Curfs, J. H. (2004) Genetic disorders of transporters/channels in the inner ear and their relation to the kidney. *Pediatr. Nephrol. 19*, 1194–1201.
9. Splawski, I., Tristani-Firouzi, M., Lehmann, M. H., Sanguinetti, M. C., and Keating, M. T. (1997) Mutations in the hminK gene cause long QT syndrome and suppress IKs function. *Nat. Genet. 17*, 338–340.
10. Long, S. B., Campbell, E. B., and Mackinnon, R. (2005) Crystal structure of a mammalian voltage-dependent Shaker family K^+ channel. *Science 309*, 897–903.
11. Mackinnon, R. (2004) Nobel Lecture. Potassium channels and the atomic basis of selective ion conduction. *Biosci. Rep. 24*, 75–100.
12. Torres, Y. P., Morera, F. J., Carvacho, I., and Latorre, R. (2007) A marriage of convenience: β-Subunits and voltage-dependent K^+ channels. *J. Biol. Chem. 282*, 24485–24489.
13. Howard, R. J., Clark, K. A., Holton, J. M., and Minor, D. L., Jr. (2007) Structural insight into KCNQ (Kv7) channel assembly and channelopathy. *Neuron 53*, 663–675.
14. Wiener, R., Haitin, Y., Shamgar, L., Fernandez-Alonso, M. C., Martos, A., Chomsky-Hecht, O., Rivas, G., Attali, B., and Hirsch, J. A. (2008) The KCNQ1 (Kv7.1) COOH Terminus, a Multitiered Scaffold for Subunit Assembly and Protein Interaction. *J. Biol. Chem. 283*, 5815–5830.
15. Tian, C., Vanoye, C. G., Kang, C., Welch, R. C., Kim, H. J., George, A. L., Jr., and Sanders, C. R. (2007) Preparation, functional characterization, and NMR studies of human KCNE1, a voltage-gated potassium channel accessory subunit associated with deafness and long QT syndrome. *Biochemistry 46*, 11459–11472.
16. Battiste, J. L., and Wagner, G. (2000) Utilization of site-directed spin labeling and high-resolution heteronuclear nuclear magnetic resonance for global fold determination of large proteins with limited nuclear overhauser effect data. *Biochemistry 39*, 5355–5365.
17. Schwieters, C. D., Kuszewski, J. J., Tjandra, N., and Clore, G. M. (2003) The Xplor-NIH NMR molecular structure determination package. *J. Magn. Reson. 160*, 65–73.
18. Smith, J. A., Vanoye, C. G., George, A. L., Jr., Meiler, J., and Sanders, C. R. (2007) Structural models for the KCNQ1 voltage-gated potassium channel. *Biochemistry 46*, 14141–14152.
19. Yarov-Yarovoy, V., Baker, D., and Catterall, W. A. (2006) Voltage sensor conformations in the open and closed states in ROSETTA structural models of K^+ channels. *Proc. Natl. Acad. Sci. U.S.A. 103*, 7292–7297.
20. Gray, J. J., Moughon, S., Wang, C., Schueler-Furman, O., Kuhlman, B., Rohl, C. A., and Baker, D. (2003) Protein-protein docking with simultaneous optimization of rigid-body displacement and side-chain conformations. *J. Mol. Biol. 331*, 281–299.
21. Tai, K. K., and Goldstein, S. A. (1998) The conduction pore of a cardiac potassium channel. *Nature 391*, 605–608.
22. Panaghie, G., Tai, K. K., and Abbott, G. W. (2006) Interaction of KCNE subunits with the KCNQ1 K^+ channel pore. *J. Physiol. 570*, 455–467.
23. Tapper, A. R., and George, A. L., Jr. (2001) Location and orientation of minK within the I(Ks) potassium channel complex. *J. Biol. Chem. 276*, 38249–38254.
24. Wang, C., Schueler-Furman, O., and Baker, D. (2005) Improved side-chain modeling for protein-protein docking. *Protein Sci. 14*, 1328–1339.
25. Choowongkomon, K., Carlin, C. R., and Sonnichsen, F. D. (2005) A structural model for the membrane-bound form of the juxtamembrane domain of the epidermal growth factor receptor. *J. Biol. Chem. 280*, 24043–24052.
26. Chou, J. J., Kaufman, J. D., Stahl, S. J., Wingfield, P. T., and Bax, A. (2002) Micelle-induced curvature in a water-insoluble HIV-1 Env peptide revealed by NMR dipolar coupling measurement in stretched polyacrylamide gel. *J. Am. Chem. Soc. 124*, 2450–2451.
27. Lee, S. Y., Lee, A., Chen, J., and Mackinnon, R. (2005) Structure of the KvAP voltage-dependent K^+ channel and its dependence on the lipid membrane. *Proc. Natl. Acad. Sci. U.S.A. 102*, 15441–15446.
28. Tapper, A. R., and George, A. L., Jr. (2000) MinK subdomains that mediate modulation of and association with KvLQT1. *J. Gen. Physiol. 116*, 379–390.
29. Dyson, H. J., and Wright, P. E. (2005) Intrinsically unstructured proteins and their functions. *Nat. Rev. Mol. Cell Biol. 6*, 197–208.
30. Furukawa, T., Ono, Y., Tsuchiya, H., Katayama, Y., Bang, M. L., Labeit, D., Labeit, S., Inagaki, N., and Gregorio, C. C. (2001) Specific interaction of the potassium channel β-subunit minK with the sarcomeric protein T-cap suggests a T-tubule-myofibril linking system. *J. Mol. Biol. 313*, 775–784.
31. Heitzmann, D., Koren, V., Wagner, M., Sterner, C., Reichold, M., Tegtmeier, I., Volk, T., and Warth, R. (2007) KCNE β subunits determine pH sensitivity of KCNQ1 potassium channels. *Cell. Physiol. Biochem. 19*, 21–32.
32. Peretz, A., Schottelndreier, H., haron-Shamgar, L. B., and Attali, B. (2002) Modulation of homomeric and heteromeric KCNQ1 channels by external acidification. *J. Physiol. 545*, 751–766.
33. Chen, H., Kim, L. A., Rajan, S., Xu, S., and Goldstein, S. A. (2003) Charybdotoxin binding in the I(Ks) pore demonstrates two MinK subunits in each channel complex. *Neuron 40*, 15–23.
34. Morin, T. J., and Kobertz, W. R. (2008) Counting membrane-embedded KCNE β-subunits in functioning K^+ channel complexes. *Proc. Natl. Acad. Sci. U.S.A. 105*, 1478–1482.
35. Chen, H., and Goldstein, S. A. (2007) Serial perturbation of MinK in IKs implies an α-helical transmembrane span traversing the channel corpus. *Biophys. J. 93*, 2332–2340.
36. Melman, Y. F., Krumerman, A., and McDonald, T. V. (2002) A single transmembrane site in the KCNE-encoded proteins controls the specificity of KvLQT1 channel gating. *J. Biol. Chem. 277*, 25187–25194.
37. Chen, J., Zheng, R., Melman, Y. F., and McDonald, T. V. (2008) C-Terminal Interactions Between KCNE1 and KCNQ1. *Biophys. J. 94*, 1382.
38. Ben Efraim, I., Bach, D., and Shai, Y. (1993) Spectroscopic and functional characterization of the putative transmembrane segment of the minK potassium channel. *Biochemistry 32*, 2371–2377.
39. Mercer, E. A., Abbott, G. W., Brazier, S. P., Ramesh, B., Haris, P. I., and Srai, S. K. (1997) Synthetic putative transmembrane region of minimal potassium channel protein (minK) adopts an α-helical conformation in phospholipid membranes. *Biochem. J. 325*, 475–479.
40. Aggeli, A., Boden, N., Cheng, Y. L., Findlay, J. B., Knowles, P. F., Kovatchev, P., and Turnbull, P. J. (1996) Peptides modeled on the transmembrane region of the slow voltage-gated IsK potassium

channel: structural characterization of peptide assemblies in the β-strand conformation. *Biochemistry 35*, 16213–16221.
41. Chung, D. Y., Chan, P. J., Karlin, A., Marx, S. O., Liu, G., and Kass, R. S. (2008) Cysteine Substitution Reveals Novel Intersubunit Interactions In The Iks Potassium Channel. *Biophys. J. 94*, 82.
42. Xu, X., Jiang, M., Hsu, K.-L., Cheng, C.-S., Zhang, M., Lyu, P.-C., and Tseng, G.-Y. (2008) KCNQ1 and KCNE1 Make State-dependent Contacts in Their Extracellular Domains. *Biophys. J. 94*, 1745.
43. Melman, Y. F., Um, S. Y., Krumerman, A., Kagan, A., and McDonald, T. V. (2004) KCNE1 binds to the KCNQ1 pore to regulate potassium channel activity. *Neuron 42*, 927–937.
44. Panaghie, G., and Abbott, G. W. (2007) The role of S4 charges in voltage-dependent and voltage-independent KCNQ1 potassium channel complexes. *J. Gen. Physiol. 129*, 121–133.
45. Arnestad, M., Crotti, L., Rognum, T. O., Insolia, R., Pedrazzini, M., Ferrandi, C., Vege, A., Wang, D. W., Rhodes, T. E., George, A. L., Jr., and Schwartz, P. J. (2007) Prevalence of long-QT syndrome gene variants in sudden infant death syndrome. *Circulation 115*, 361–367.
46. Bianchi, L., Priori, S. G., Napolitano, C., Surewicz, K. A., Dennis, A. T., Memmi, M., Schwartz, P. J., and Brown, A. M. (2000) Mechanisms of I(Ks) suppression in LQT1 mutants. *Am. J. Physiol. 279*, H3003–H3011.
47. Hong, K., Piper, D. R., az-Valdecantos, A., Brugada, J., Oliva, A., Burashnikov, E., Santos-de-Soto, J., Grueso-Montero, J., az-Enfante, E., Brugada, P., Sachse, F., Sanguinetti, M. C., and Brugada, R. (2005) De novo KCNQ1 mutation responsible for atrial fibrillation and short QT syndrome in utero. *Cardiovasc. Res. 68*, 433–440.
48. Nakajo, K., and Kubo, Y. (2007) KCNE1 and KCNE3 stabilize and/or slow voltage sensing S4 segment of KCNQ1 channel. *J. Gen. Physiol 130*, 269–281.
49. Rocheleau, J. M., and Kobertz, W. R. (2008) KCNE peptides differently affect voltage sensor equilibrium and equilibration rates in KCNQ1 K^+ channels. *J. Gen. Physiol. 131*, 59–68.
50. Rocheleau, J. M., Gage, S. D., and Kobertz, W. R. (2006) Secondary structure of a KCNE cytoplasmic domain. *J. Gen. Physiol. 128*, 721–729.

BI800875Q